IEEE Access
Multidisciplinary | Rapid Review | Open Access Journal

Received September 29, 2021, accepted October 21, 2021, date of publication October 26, 2021,
date of current version November 8, 2021.

Digital Object Identifier 10.1109/ACCESS.2021.3122837

Phase-Only Space-Time Adaptive Processing

LUCA PALLOTTA[1], (Senior Member, IEEE), ALFONSO FARINA[2], (Life Fellow, IEEE), STEVEN THOMAS SMITH[3], (Fellow, IEEE), AND GAETANO GIUNTA[1], (Senior Member, IEEE)

[1]Industrial, Electronics, and Mechanical Engineering Department, University of Roma Tre, 00146 Rome, Italy
[2]Selex ES, 00131 Rome, Italy *(retired)*
[3]Lincoln Laboratory, Massachusetts Institute of Technology, Lexington, MA 02421, USA

Corresponding author: Luca Pallotta (luca.pallotta@uniroma3.it)

This material is based upon work supported by the Under Secretary of Defense for Research and Engineering under Air Force Contract No. FA8702-15-D-0001. Any opinions, findings, conclusions or recommendations expressed in this material are those of the author(s) and do not necessarily reflect the views of the Under Secretary of Defense for Research and Engineering. The work of Luca Pallotta and Gaetano Giunta is funded by University of Roma Tre.

ABSTRACT Space-time adaptive processing (STAP) is a well-known and effective method to detect targets, obscured by interference, from airborne radars that works by coherently combining signals from a phased antenna array (spatial domain) with multiple radar pulses (temporal domain). As widely demonstrated, optimum STAP, in the sense of maximizing the output signal to interference plus noise ratio (SINR), is a coherent, linear, transversal filter (i.e., tapped delay line), that can be synthesized by a complex-valued weight vector. This paper extends previous work that focused on adaptive spatial-only nulling; it derives the optimum phase-only STAP, namely, the optimal weight vector that maximizes the SINR subject to the constraint it belongs to the N-torus of phase-only complex vectors, where N is the number of spatio-temporal degrees of freedom. Because this problem does not admit a closed-form solution, it is solved numerically using the phase-only conjugate gradient method (CGM). The effectiveness of phase-only STAP is demonstrated using both SINR values and receiving beampattern shape, comparing it with the optimum fully-adapted STAP and the nonadapted beam former responses as well as other possible counterparts. Additionally, several analyses of practical utility also demonstrate the benefits provided by phase-only STAP.

INDEX TERMS Radar signal processing, space time adaptive processing (STAP), adaptive radar receiver, phase-only adaptive nulling, phase-only STAP, gradient descent method.

I. INTRODUCTION

Radar space-time adaptive processing (STAP) is a powerful technique used in airborne systems to detect a target embedded in interference potentially comprising clutter, jamming and noise [1]–[5]. More in details, STAP is the processor capable of jointly combining the signals acquired by multiple antenna's elements of a phased-array, indicated as the spatial or angular domain, and in a coherent processing interval (CPI) composed by multiple pulse repetition intervals (PRIs), that is the temporal or Doppler domain [2]. By doing so, even if the target is indistinguishable in a single space or time domain, it would be visible (and hence detected, tracked and classified) in the joint space-time domain [2], [4]. It is worth highlighting that STAP can be seen as a two-dimensional (2-D) filter jointly combining beamforming and Doppler filtering [2]. In particular, it should be observed first that in analyzing the detection capabilities of a radar system it is essential to take into account the signal to interference plus noise ratio (SINR) that provides a measure of the radar strength to distinguish the target component with respect to the interferences in the received signal. Therefore, assuming a radar transmitting a coherent pulse train through a phased-array antennas, it should be proved (see [6] for more details) that the processor that maximizes the output SINR is a coherent, linear, transversal filter.

Due to the primary role of this processing in airborne radars,[1] exhaustive technical literature has been published on this interesting and challenging topic aimed at improving several characterizing aspects [9]. Methodologies for the on-line computation of the weight vectors in STAP have been proposed and some applied in practice in [10]–[14]. These methods exploit computationally efficient techniques as well as lattice-based algorithms to obtain a variety of adapted beam focused on different directions and Doppler frequencies and, at the same time, strongly reducing the computational

The associate editor coordinating the review of this manuscript and approving it for publication was Hasan S. Mir.

[1]STAP finds application to also other contexts such as to synthetic aperture radar (SAR) processing [7], [8].

burden towards real-time implementations. Moreover, several studies have been conducted to demonstrate the effectiveness of the radar STAP in such environments that go beyond the classic homogeneous assumption [15]–[19]. For instance, in [18], space-time models for both amplitude and spectral clutter heterogeneity are proposed and the losses experienced by STAP have been evaluated under these circumstances. Then, in [20] optimal and adaptive reduced-rank (both two- and three-dimensional) STAP algorithms for joint hot and cold clutter mitigation are provided. Analogously, also in [21] some applications of reduced-rank methods for STAP have been described and deeply analyzed. Again, some works, e.g. [22]–[25], have investigated the potential exploitation of some a-priori information about the disturbance covariance to improve the radar STAP detection capabilities. Moreover, in [26] a partially adaptive STAP based on the so-called FRACTA (a reiterative censoring and detection procedure) algorithm is implemented aimed at reducing the computational complexity as well as the required sample support. Other developments have been provided in [27], where the authors propose a code design algorithm based on the maximization of the detection performance of a radar STAP controlling the regions of achievable values for the temporal and spatial Doppler estimation accuracy, as well as the degree of similarity with a pre-fixed radar code. Moreover, [28] models the disturbance as a low-rank spherically invariant random vector (SIRV) clutter plus a zero-mean white Gaussian noise and proposes a STAP algorithm framed within this context exploiting the projection of the estimate in the clutter subspace. In [29], a robust adaptive beamforming is developed in the presence of some mismatches in the desired signal and the disturbance covariance for a factored radar STAP. Beyond STAP, some interesting developments can be found in [30]–[34], where a joint design of transmit waveform and receive filter is performed using the output SINR as objective function.

All the above-mentioned research papers are essentially based on the computation of the weight vector, that for the optimum adapted radar STAP (i.e., that maximizing the SINR) is essentially described by a number of complex quantities that would be multiplied to the received signal samples in the receiving filter. However, in several practical implementations, the radar receiver could comprise only phase shifters not-always sharing also amplitude tuners; therefore, it would be interesting to implement complex weights having a constant modulus, namely to derive a phase-only weight vector. This problem has been addressed in [35], where the optimum phase-only adaptive array has been designed formalizing the problem as a SINR maximization constraining the weight vectors to belong to the phase-only space. The problem has been solved thanks to two different algorithms that are the phase-only conjugate gradient method (CGM) and the Newton's method. This paper addresses the problem of optimum phase-only STAP, extending the work focused on phase-only adaptive spatial nulling of [35] filling the gap towards the radar STAP. The idea is to find the STAP weight vector maximizing the SINR constraining it to belong to the space of phase-only vectors. As in [35], also in this case the problem does not admit a closed-form solution, and it is solved resorting to the phase-only CGM. Even if the considered method provides only a local maximization of the SINR, a proper selection of the starting point allows to reach near-optimum performance. The effectiveness of the phase-only STAP is shown in the analysis section, evaluating the receiving beampattern shape, the achievable SINR, and the sidelobes level of the adapted two-dimensional beam also in comparison with the optimum adapted STAP as well as to other possible counterparts. An analysis of the phase behavior, also in the presence of a limited number of bits to code them, is performed to highlight the effectiveness of this method also in practical situations. Additionally, the fully-adapted phase-only STAP architecture is analyzed to verify the validity of the Reed-Mallet-Brennan rule [36]. Finally, a method for jointly optimizing the transmitted waveform and the receiving filter, constraining both of them to be phase-only vectors, is also provided.

Summarizing, the main contributions of this paper are:

- the derivation of the optimum phase-only STAP extending a previous work that focused on adaptive spatial-only nulling;
- extensive analyses of the phase-only STAP in several interfering scenarios of interest and to practical implementation tests;
- the application of the method for jointly optimizing the transmitted waveform and the receiving filter, constraining both of them to be phase-only vectors.

The paper is organized as follows. Section II briefly recalls the STAP concept, introduces the formalism together with the description of the considered radar architecture. Then, Section III presents the phase-only STAP and provides the description of the used solution based on the CGM. The performance analyses are conducted and discussed in Section IV. Conclusions and suggestions for possible future developments are given in Section V.

Notation:

We use boldface for vectors $\boldsymbol{a}$ (lower case) and matrices $\boldsymbol{A}$ (upper case). The transpose and the conjugate transpose operators are denoted by the symbols $(\cdot)^T$ and $(\cdot)^\dagger$ respectively. $\mathbf{Diag}\,(\boldsymbol{a})$ is the diagonal matrix whose i-th diagonal element is the i-th entry of $\boldsymbol{a}$, whereas $\mathbf{diag}(\boldsymbol{A})$ is the diagonal part of the matrix $\boldsymbol{A}$. $\boldsymbol{I}$ refers to the identity matrix (its size is determined from the context). $\mathbb{C}^N$ and $\mathbb{T}^N$ are the sets of N-dimensional vectors of complex numbers and elements of the phase-only torus, respectively. The symbols $\otimes$ and $\odot$ indicate the Kronecker and the element-wise or Hadamard product, respectively. The letter j represents the imaginary unit (i.e. $j = \sqrt{-1}$). For any complex number x, $|x|$ indicates its modulus, and $\mathrm{Im}\{x\}$ indicates its imaginary part. The Frobenius matrix norm is denoted by $\|\cdot\|$, and $\mathbb{E}[\cdot]$ is statistical expectation. Finally, $[\boldsymbol{A}, \boldsymbol{B}]$ between matrices $\boldsymbol{A}$ and $\boldsymbol{B}$ is the Lie bracket or commutator product defined as $\boldsymbol{AB} - \boldsymbol{BA}$.

II. OPTIMUM SPACE-TIME ADAPTIVE PROCESSING

This section formalizes the concept of space-time adaptive processing together with the description of the respective optimum radar receive filter. To do this a pulse-Doppler radar comprising L spatial channels and transmitting M coherent pulses is taken into account. Hence, the radar antenna is a uniformly spaced linear array antenna (ULA) consisting of L elements. Indicating with θ the azimuth angle variable, the spatial steering is given by

$$\boldsymbol{v}_s(\theta) = \left[1, e^{j\phi\sin(\theta)}, \ldots, e^{j\phi(L-1)\sin(\theta)}\right]^T, \tag{1}$$

having implicitly assumed that the space between antenna's elements is equal to $d = \lambda_0/2$, with λ_0 the radar operating wavelength. The radar is assumed to transmits a coherent train of M pulses at regular pulse repetition interval (PRI), say T. Therefore, indicating with ν_D the frequency variable representing the Doppler frequency normalized to PRF $= 1/T$, the temporal steering is

$$\boldsymbol{v}_t(\nu_D) = \left[1, e^{j2\pi\nu_D}, \ldots, e^{j2\pi(M-1)\nu_D}\right]^T. \tag{2}$$

Then, the joint spatio-temporal steering vector of size $N = ML$ is defined to be

$$\boldsymbol{v}(\nu_D, \theta) = \boldsymbol{v}_t(\nu_D) \otimes \boldsymbol{v}_s(\theta). \tag{3}$$

For sake of brevity, in what follows, the dependence of $\boldsymbol{v}$ on ν_D and θ will be omitted. Let us now denote by

$$\boldsymbol{r} = \boldsymbol{v} + \boldsymbol{n} \tag{4}$$

the N-dimensional vector associated to the received signal of the cell under test, where $\boldsymbol{n}$ is the zero-mean vector associated to the disturbance components. Then, it can be demonstrated that the optimum filter output is given by the inner product between the weight vector and the useful signal, namely

$$s = \boldsymbol{w}^\dagger \boldsymbol{r}, \tag{5}$$

where $\boldsymbol{w} \in \mathbb{C}^N$ is the complex N-dimensional weight vector.

Moreover, denoting by $\mathbb{E}[\boldsymbol{n}\boldsymbol{n}^\dagger] = \boldsymbol{M}$ the unknown disturbance (viz. clutter plus directional interference plus noise) covariance matrix, the SINR at the output of the above mentioned filter is

$$\text{SINR} = \frac{\left|\boldsymbol{w}^\dagger \boldsymbol{v}\right|^2}{\boldsymbol{w}^\dagger \boldsymbol{M} \boldsymbol{w}} \tag{6}$$

It can be shown that the SINR described in (6) attains its maximum when the weight vector is chosen as

$$\boldsymbol{w} = \boldsymbol{M}^{-1}\boldsymbol{v}, \tag{7}$$

that is typically referred to as the optimum radar receiver filter [2], [3] whose schematic representation is given in Figure 1. As it can be clearly observed from (7), the optimum receiving filter for STAP essentially assumes the knowledge of the steering vector $\boldsymbol{v}$ and requires the computation of the disturbance covariance matrix. Conversely, a phase-only adaptive radar STAP is based on the computation of the complex weights that are described by only a phase term and that maximizes the SINR in (6). A direct method to estimate the optimum phase-only weight vector does not exist and requires the use of gradient-based methods. In the next section, following the same line of reasoning of [35], an effective method based on the Hestenes and Stiefel's conjugate gradient algorithm [37] is derived.

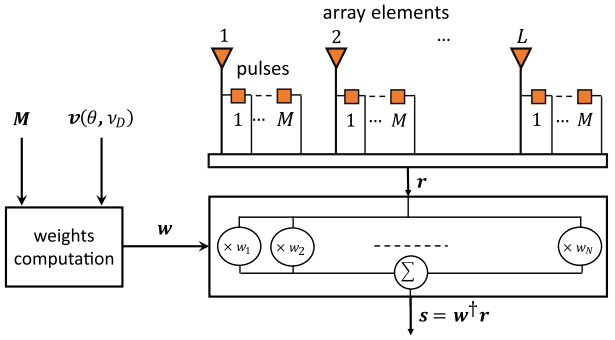

FIGURE 1. Block scheme of the optimum STAP receiver.

III. OPTIMUM PHASE-ONLY STAP

The *optimum adaptive* STAP radar is based on the use of the disturbance covariance matrix in the filter design arising from maximizing the SINR over all possible complex vectors of size N, viz. $\boldsymbol{w} \in \mathbb{C}^N$. The *Phase-only* STAP tries to estimate the complex vectors $\boldsymbol{w}$ constraining its elements to have unit amplitude, that is the complex weight vectors is enforced assuming the following form

$$\boldsymbol{w} = \left[e^{j\phi_1}, e^{j\phi_2}, \ldots, e^{j\phi_N}\right]^T. \tag{8}$$

Therefore, the phase-only weight vector is obtained as the solution to the following optimization problem

$$\mathcal{P}\begin{cases} \boldsymbol{w}_{\text{PO}} = \arg\max_{\boldsymbol{w}} \left(\dfrac{\left|\boldsymbol{w}^\dagger \boldsymbol{v}\right|^2}{\boldsymbol{w}^\dagger \boldsymbol{M} \boldsymbol{w}}\right) \\ \text{s.t. } \boldsymbol{w} \in \mathbb{T}^N, \end{cases} \tag{9}$$

namely as the vector maximizing the SINR over the N-torus. As already said this paper extends a previous work that focused on adaptive spatial-only nulling [35] to the more general framework of STAP. As highlighted in [35], the phase-only case does not admit a closed-form solution to the constrained optimization problem. The identical challenge exists for phase-only STAP because, unlike the fully optimal case, there is not a closed-form solution to Eq. (9). This is pictorially represented in Figure 2 for a phase-only STAP weight composed by only two array elements transmitting two radar pulses. The space of a phase-only element comprising two antenna elements and two pulses cannot be visually represented because of the four involved phases, however it can be graphically drawn by means of an unfolded torus (which is a projection of the SINR from the space of the four phases in a three-dimensional space in which the

variation is due to only two phases), representing the SINR variation with respect to ϕ_2 and ϕ_3 having set, in this case, $\phi_4 = 0$ and $\phi_1 = [0, \pi/4, \pi/2]$. The unfolded torus clearly emphasizes the presence of many maxima in the overall N-torus and the consequent impossibility in finding a closed-form optimal solution. For these reasons in the following phase-only STAP is solved by introducing a generalization of the CGM provided in [35] to this specific problem. The phase-only STAP can be represented by means of the block scheme of Figure 3 in which the differences with the optimum adapted STAP are clearly either evident. Precisely, the weight vector is computed applying the CGM as described in the following, and then the signal's samples are phase shifted by the amount of tuning contained by the optimal phase-only weights.

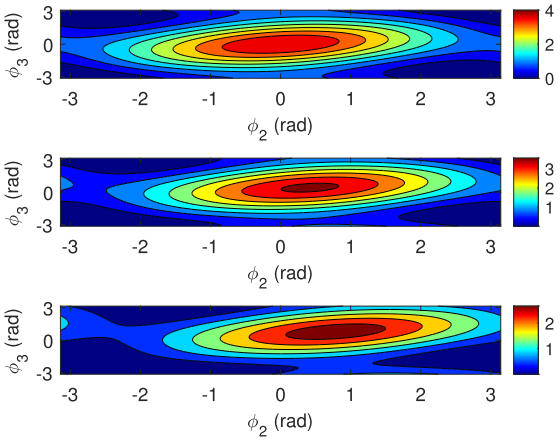

FIGURE 2. Phase-only SINR for a two-elements two-pulses STAP with respect to the phases of the phase-only weight vector $w \in \mathbb{T}^N$. The figure refers to the SINR variation with respect to ϕ_2 and ϕ_3 having set $\phi_4 = 0$ and for $\phi_1 = [0, \pi/4, \pi/2]$, respectively from top to bottom.

To simplify the mathematical derivations as well as to easily distinguish the phase-only SINR from the fully-adapted, this latter is expressed as

$$\text{SINR}_{\text{PO}} = \sigma(\boldsymbol{w}) = \frac{\boldsymbol{w}^\dagger \boldsymbol{S} \boldsymbol{w}}{\boldsymbol{w}^\dagger \boldsymbol{M} \boldsymbol{w}}, \quad \boldsymbol{w} \in \mathbb{T}^N, \tag{10}$$

with $\boldsymbol{w}$ defined in (8) obtained as the solution to (9) and $\boldsymbol{S} = \boldsymbol{v}\boldsymbol{v}^\dagger$.

Before proceeding further, some considerations about the phase-only strategy will be discussed. In particular, it is worth recalling that some other solutions for adaptive radar based on the exploitation of the Lagrange multipliers or utilizing a specific modification of the eigenvalue analysis of the weight vector can be found [38, p. 286], [39]. These methods can be solved through iterative minimization algorithms such as random search or simplex method, even if they might be inefficient and computationally expensive. Therefore, as in [35], the phase-only STAP problem is solved by means of an innovative optimization algorithm that is the phase-only CGM, obtained by adapting Riemannian optimization methods [40]–[43] to this context. Because this algorithm is based on the evaluation of the gradient of the SINR, in the following subsection the Taylor series expansion of the phase-only SINR derived in [35] is included.

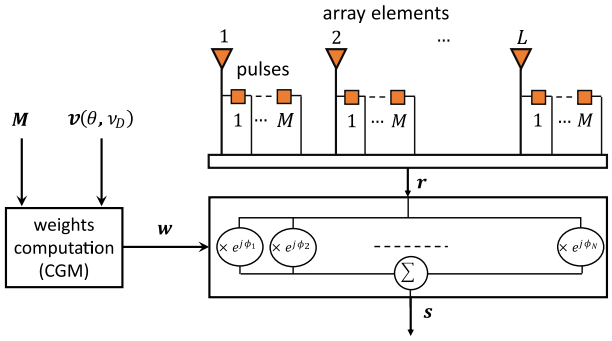

FIGURE 3. Block scheme of the optimum phase-only STAP receiver.

A. PHASE-ONLY SINR'S TAYLOR EXPANSION AND GRADIENT COMPUTATION

In this subsection the phase-only SINR's Taylor expansion for STAP is provided in order to allows the derivation of the phase-only SINR gradient. It is worth noticing that the SINR of a phase-only STAP has the same structural form to that of a spatial-only adaptive array radar. Nevertheless, it must be noted that all the involved quantities (viz. steering vector, weight vector, and covariance matrix) differ in form from their spatial-only counterparts. After this premise, in the following the main steps involved in the derivation of the SINR's Taylor series are provided. However, the interested readers can refer to [35] for all mathematical derivations and proofs.

Consider the effect of small phase perturbations on the phase-only weight vector $\boldsymbol{w}$, that is,

$$\boldsymbol{w} \to e^{j\boldsymbol{\Delta}} \boldsymbol{w}, \tag{11}$$

where $\boldsymbol{\Delta} = \textbf{Diag}\,([\delta_1, \ldots, \delta_N])$, with $\delta_1, \ldots, \delta_N$ the perturbations of the phases $\phi_1, \ldots, \phi_N$.

Now, the SINR in (10) can be separately treated in its numerator $N(\boldsymbol{w})$ and denominator $D(\boldsymbol{w})$, whose perturbed versions are $N(e^{j\boldsymbol{\Delta}t}\boldsymbol{w}) = \boldsymbol{w}^\dagger e^{-j\boldsymbol{\Delta}t} \boldsymbol{S} e^{j\boldsymbol{\Delta}t} \boldsymbol{w}$ and $D(e^{j\boldsymbol{\Delta}t}\boldsymbol{w}) = \boldsymbol{w}^\dagger e^{-j\boldsymbol{\Delta}t} \boldsymbol{M} e^{j\boldsymbol{\Delta}t} \boldsymbol{w}$, respectively. Then, the Taylor expansion series for the numerator and the inverse of the denominator is given by [35]

$$N(e^{j\boldsymbol{\Delta}t}\boldsymbol{w}) = \boldsymbol{w}^\dagger \left(\boldsymbol{S} - j[\boldsymbol{\Delta}, \boldsymbol{S}] - (1/2)\,[\boldsymbol{\Delta}, [\boldsymbol{\Delta}, \boldsymbol{S}]] + \ldots\right) \boldsymbol{w} \tag{12}$$

and

$$\begin{aligned} \frac{1}{D(e^{j\boldsymbol{\Delta}t}\boldsymbol{w})} = {} & \frac{1}{\boldsymbol{w}^\dagger \boldsymbol{M} \boldsymbol{w}} \\ & + \boldsymbol{w}^\dagger \left(j[\boldsymbol{\Delta}, \boldsymbol{M}] + \frac{1}{2}\,[\boldsymbol{\Delta}, [\boldsymbol{\Delta}, \boldsymbol{M}]] \right) \frac{\boldsymbol{w}}{\left(\boldsymbol{w}^\dagger \boldsymbol{M} \boldsymbol{w}\right)^2} \\ & - \frac{\left(\boldsymbol{w}^\dagger [\boldsymbol{\Delta}, \boldsymbol{M}] \boldsymbol{w}\right)^2}{\left(\boldsymbol{w}^\dagger \boldsymbol{M} \boldsymbol{w}\right)^3} + \ldots \end{aligned} \tag{13}$$

The gradient can be directly computed as shown in the following.

The gradient of $\sigma(\boldsymbol{w})$ is obtained as the ratio

$$\sigma\left(e^{j\boldsymbol{\Delta}}\boldsymbol{w}\right) = N\left(e^{j\boldsymbol{\Delta}}\boldsymbol{w}\right)/D\left(e^{j\boldsymbol{\Delta}}\boldsymbol{w}\right), \tag{14}$$

where the numerator and the inverse of denominator are given in (12) and (13), respectively. Then, extracting the first order terms of the Taylor series expansion with respect to $\boldsymbol{\Delta}$, and after some algebraic manipulations, the gradient becomes

$$\nabla\sigma(\boldsymbol{w}) = \frac{1}{\boldsymbol{w}^{\dagger}\boldsymbol{M}\boldsymbol{w}}\mathrm{Im}\left\{\mathbf{diag}\left([\boldsymbol{S} - \sigma(\boldsymbol{w})\boldsymbol{M}, \boldsymbol{w}\boldsymbol{w}^{\dagger}]\right)\right\}. \tag{15}$$

Exploiting the property that the phase-only SINR is invariant under the transformation $\boldsymbol{w} \to e^{j\theta}\boldsymbol{w}$, its gradient in (15) can be computed as [35]

$$\nabla\sigma(\boldsymbol{w}) = 2\left(\mathrm{Im}\left(\alpha^{*}\boldsymbol{v}\odot\boldsymbol{w}^{*}\right) - \sigma(\boldsymbol{w})\mathrm{Im}\left(\boldsymbol{b}\odot\boldsymbol{w}^{*}\right)\right)/\gamma, \tag{16}$$

where $\alpha = \boldsymbol{w}^{\dagger}\boldsymbol{v}$, $\boldsymbol{b} = \boldsymbol{M}\boldsymbol{w}$, and $\gamma = \boldsymbol{w}^{\dagger}\boldsymbol{b}$. It is worth to note here that, even if from a structural point-of-view (16) is equal to (32) in [35], the involved quantities significantly differ in the two equations.

B. CONJUGATE GRADIENT METHOD FOR PHASE-ONLY STAP

Having derived the SINR's gradient in the previous subsection, it can be now properly used to solve the optimization problem $\mathcal{P}$ in (9) through algorithms based on the exploitation of first-order derivatives. Therefore, following the line of reasoning of [35], the CGM [44, p. 625] is applied optimizing on lines on the N-torus in place of lines in the Euclidean space, that is

$$\boldsymbol{w} + t\boldsymbol{d} \to e^{jt\mathbf{Diag}(\boldsymbol{d})}\boldsymbol{w}, \tag{17}$$

where $\boldsymbol{w}$ is the phase-only weight vector, $\boldsymbol{d}$ is the direction, and t is the step size. Note that, the structure of the lines in the N-torus space in (17) derive from the fact that the involved perturbations of the weight vector act on its phases.

The CGM for computing phase-only optimum weights for STAP radars can be summarized by the steps described in Algorithm 1.

The algorithm starts with the initialization of the phase-only weight vector $\boldsymbol{w}_0$, i.e. belonging to the N-torus. It is here worth to recall that the phase-only SINR shares many local maximum, as can be observed from the simplest case depicted in Figure 2. As a consequence, the method is strongly influenced by its initial point, that can be set for simplicity as the optimal choice in the quiescent STAP, $\boldsymbol{w}_0 = \boldsymbol{v}$. The convergence of this algorithm for the computation of phase-only weights has already be proved by simulation in [35], therefore in the Section IV we directly exploits those results. Nevertheless, different initializations of the algorithm can be considered. In particular, an alternative initializer could consist in the use of the clairvoyant target spatial steering vector of size L with a random Doppler steering vector of size M drawn from some suitable distribution or the clairvoyant target Doppler steering vector of size M with a random spatial steering vector of size M. The robustness of the CGM algorithm with respect to the initialization point is studied in Section IV. The other point that merits some further clarifications is that regarding the step size evaluation $t_i^{\star}$. In fact, the considered searching problem is framed within the context of geometric algorithms. It consists in defining a line or, in this case, a geodesic on the torus and efficiently searching for the maximum (or minimum) along it (viz., 1D optimization along the line). This can be done utilizing many line search algorithms, as for instance Wolf-Powell. See [40], [43] in the context in geometric algorithms. As to the computational complexity required by Algorithm 1, note that to compute the updated search direction d_{i+1} it requires $2ML$ real floating-point operations (flops). Moreover, each iteration requires $8M^2L^2$ flops for matrix-vector multiplication and $27ML$ flops to compute the gradient (without the computation for $\boldsymbol{M}\boldsymbol{w}$). Finally, in practical context, the covariance estimation is made with $4KM^2L^2$ flops, with K the number of snapshots used in the estimation process.

To conclude, the Newton's method could be also applied in this context. However, from a structural point of view, its formalization for the phase-only STAP is the same as

Algorithm 1 Conjugate Gradient Method for Phase-Only STAP

Input: Disturbance covariance matrix $\boldsymbol{M}$, and space-time steering vector $\boldsymbol{v}(\nu_D, \theta)$;

Output: Optimum phase-only weight vector $\boldsymbol{w}_{\mathrm{PO}}$;

1: Initialization ($i = 0$): set $\boldsymbol{w}_0 \in \mathbb{T}^N$ (see below); then, compute $\boldsymbol{g}_0 = \nabla\sigma(\boldsymbol{w})$ through (16) and set $\boldsymbol{d}_0 = \boldsymbol{g}_0$;
2: **for** $i = 1$ **to** $i = i_{\max}$ **do**
3: Line optimization: compute t_i that maximizes the phase-only constrained SINR, that is

$$t_i^{\star} = \arg\max_{t_i \geq 0}\left\{\sigma\left(e^{jt_i\mathbf{Diag}(\boldsymbol{d}_i)}\boldsymbol{w}_i\right)\right\};$$

4: Compute the weight vector at the next step, that is

$$\boldsymbol{w}_{i+1} = e^{jt_i^{\star}\mathbf{Diag}(\boldsymbol{d}_i)}\boldsymbol{w}_i;$$

5: Compute the gradient and direction at the next step, that is

$$\boldsymbol{g}_{i+1} = \nabla\sigma(\boldsymbol{w}_{i+1}),$$
$$\gamma_i = \frac{\left(\boldsymbol{g}_{i+1} - \boldsymbol{g}_i\right)^T\boldsymbol{g}_{i+1}}{\|\boldsymbol{g}_i\|^2},$$

and

$$\boldsymbol{d}_{i+1} = \boldsymbol{g}_{i+1} + \gamma_i\boldsymbol{d}_i;$$

6: **if** $i \equiv N - 1 \pmod N$ **then**
7: Reset the CGM: set $\boldsymbol{d}_{i+1} = \boldsymbol{g}_{i+1}$.
8: **end if**
9: **end for**
10: Choose the final phase-only weight vector: $\boldsymbol{w}_{\mathrm{PO}} = \boldsymbol{w}_{i_{\max}}$.

the adaptive array in [35], in this paper we omit this discussion, inviting the interested readers to deepen the works in [35], [45].

IV. PHASE-ONLY STAP PERFORMANCE

This section is devoted to the analysis of the phase-only STAP described in Section III whose solution is found by means of the CGM given in subsection III-B. First, tests are conducted on simulated data analyzing the SINR at the space-time filter output and the corresponding receiving normalized beampattern (i.e., the radar angular-Doppler response) when the second-order interference statistics are perfectly known. Furthermore, the more realistic case of unknown covariance matrix is then considered to verify the validity of the Reed-Mallet-Brennan rule [36] for the phase-only STAP. Finally, the impact of a limited number of available bits to represent the quantized phases is also studied.

A. SINR AND BEAMPATTERN EVALUATION FOR KNOWN INTERFERENCE

The SINR at the space-time filter output is adopted as a performance metric considering the fully adaptive STAP and the quiescent beampattern (also referred to as nonadapted beam former) for comparison purposes. The radar system is a uniform linear array (ULA) of L elements with spacing between the antennas of $d = \lambda_0/2$, where λ_0 is the radar operating wavelength.

The SINR is given in (6), whereas the beampattern is defined as

$$\mathrm{BP} = \left| \boldsymbol{w}^{\dagger} \boldsymbol{v}(\nu_D, \theta) \right|^2 . \tag{18}$$

The inference scenario comprises several contributions associated with different interference sources: system noise, clutter (associated with the echoes from the specific operating environment), and jammers (intentional disturbances impinging on the radar antennas). Therefore, the interference covariance matrix is given by [2]

$$\boldsymbol{M} = \boldsymbol{M}_C + \boldsymbol{M}_J + \sigma_n^2 \boldsymbol{I},$$

where $\boldsymbol{M}_C$ is the covariance associated with clutter components, $\boldsymbol{M}_J$ the matrix accounting for jammers, and σ_n^2 is the actual system noise power level assumed uncorrelated. The clutter covariance matrix is

$$\boldsymbol{M}_C = \sigma_C^2 \boldsymbol{M}_{Ct} \otimes \boldsymbol{M}_{Cs}, \tag{19}$$

where the temporal component is Gaussian shaped

$$\begin{aligned} \boldsymbol{M}_{Ct}(h,l) &= \rho_{Ct}^{|h-l|^2} e^{j2\pi(h-l)\nu_{D_C}}, \\ & h = 1, \ldots, M,\ l = 1, \ldots, M, \end{aligned} \tag{20}$$

and the spatial component is exponentially shaped

$$\begin{aligned} \boldsymbol{M}_{Cs}(h,l) &= \rho_{Cs}^{|h-l|}, \\ & h = 1, \ldots, L,\ l = 1, \ldots, L, \end{aligned} \tag{21}$$

with σ_C^2 the clutter power, ν_{D_C} the normalized clutter Doppler frequency, and ρ_{Ct} and ρ_{Cs} the clutter temporal and spatial correlation coefficients, respectively.

The jammer covariance matrix is

$$\boldsymbol{M}_J = \sigma_J^2 \boldsymbol{I} \otimes \left(\boldsymbol{v}_J(\theta_J) \boldsymbol{v}_J(\theta_J)^{\dagger} \right), \tag{22}$$

with σ_J^2 being the jammer power, θ_J the angle off boresight of the jammer, and $\boldsymbol{v}_J$ the jammer steering defined as in (1).

The first study refers to a radar system comprising $L = 8$ antennas and transmitting a coherent burst of $M = 8$ pulses. The target echo impinges on the radar receiver with a direction of arrival (DOA) equal to $\theta_{tg} = 25$ degrees and moving towards the radar with a normalized Doppler of $\nu_{D_{tg}} = 0.4$. The interfering environment is characterized by the parameter values summarized in Table 1.

TABLE 1. Parameters of the interfering scenario for the first study case.

σ_n^2	σ_C^2	ν_{D_C}	ρ_{Ct}	ρ_{Cs}	σ_J^2	θ_J
0 dB	40 dB	0	0.95	0.95	40 dB	50 degrees

Figure 4 reports the normalized beampattern of the phase-only STAP also in comparison with those of the fully-adapted STAP, the nonadapted STAP, the phase-only in temporal domain, $\boldsymbol{w}_{\mathrm{PO},t} = \boldsymbol{w}_t \otimes \boldsymbol{v}_s$ (with $\boldsymbol{w}_t$ the optimum phase-only temporal weight vector), the phase-only in spatial domain, $\boldsymbol{w}_{\mathrm{PO},s} = \boldsymbol{v}_t \otimes \boldsymbol{w}_s$ (with $\boldsymbol{w}_s$ the optimum phase-only spatial weight vector), the phase-only evaluated in the two disjoint domains, $\boldsymbol{w} = \boldsymbol{w}_t \otimes \boldsymbol{w}_s$, the phase of the fully adaptive filter, $\boldsymbol{w}_{\mathrm{FA,phase}} = e^{j\angle \boldsymbol{M}^{-1}\boldsymbol{v}}$, and the semidefinite relaxation (SDR) method of [46]. Additionally, the interference power is also plotted so as to have a complete frame of the effectiveness of the considered approach. The pictures reveal that the phase-only STAP is capable to concentrate the power of the main-lobe in correspondence of the target position in terms of both angle and normalized Doppler (target position is indicated with the black x in the 2-D patterns). Additionally, phase-only STAP is capable of properly canceling the interference contribution by placing deep nulls in correspondence of them, as can be seen by comparing that figure with the interference power of subplot d). Comparing subplots a) and b) it is quite evident that phase-only STAP exhibits a reduced performance degradation with respect to the fully optimum STAP. From inspection of subplots d) and e), it is quite evident that the spatial and temporal phase-only alone do not give satisfactorily performances in the joint domain, i.e., if a proper cancellation is performed in the interfering angular direction, it is not done for Doppler frequency and vice-versa. Some improvements are however given by using the disjoint phase-only STAP, even if it is not able to reach the same performance as the phase-only STAP directly derived in the joint domain. Again, subplot g) demonstrates that the filter based on the phases of the fully adapted have some performance degradation with respect the fully adapted one essentially confined to the missing cancellation of the

spatial jammer. Finally, subplot e) is related to the SDR which is quite capable of correctly point towards the target and putting deep nulls in the direction/Doppler of interference, even if its shape is not very close to that of the fully adapted in some zones of the angle/Doppler map. Finally, as is well known, the unadapted filter cannot remove the interference despite correctly pointing towards the target.

To further understand the behavior of the proposed phase-only STAP, Figure 5 depicts the SINR values (expressed in dB) in the angle-Doppler map for the same interfering scenario as in Figure 4. The figures show some performance losses in the phase-only STAP with respect to the fully-adapted that can be essentially motivated by the fact that the steering points at $v_{D_{tg}} = 0.4$, $\theta_{tg} = 25$ degrees. Conversely, considering the target impinging on the radar from direction 0 degrees with 0 Doppler embedded in interference described by the covariance $\boldsymbol{M} = \boldsymbol{M}_J + \sigma_n^2 \boldsymbol{I}$ (with $\boldsymbol{M}_J$ and σ_n^2 defined as above), as given in Figure 6, the phase-only and fully-adapted STAP reach exactly the same SINRs.

To better emphasize the effectiveness of the phase-only STAP a clutter model comprising clutter edge is also considered in the next simulation. Precisely, Fig. 7 shows the beampattern for the phase-only and optimum adapted STAP assuming the target located at 0 degrees in azimuth with a normalized Doppler frequency of 0.33 and for the interfering scenario whose relative power is illustrated in Fig. 7(c). The interfering scenario is the same as in Fig. 23 of [2], where two jammers are considered having azimuth angles equal to -40 degrees and 25 degrees, respectively, whereas the stationary clutter is modeled as composed by 360 patches. The considered radar system is composed by an array of 18 elements transmitting a burst of 18 pulses in a coherent processing interval (CPI). From the figure, the capability of the phase-only STAP to put nulls in the jammers and clutter directions/Doppler is clear, at the same time maintaining undistorted the mainbeam in the target direction.

Before concluding the analysis in terms of beampatterns of this subsection, it is of interest to analyze the robustness of the CGM algorithm applied to phase-only STAP for different initialization points. In particular, we compare the beampattern of the phase-only STAP initialized with the steering $\boldsymbol{v}$ with those initialized with $\boldsymbol{w}_0 = \boldsymbol{x}_t \otimes \boldsymbol{v}_s$ and $\boldsymbol{w}_0 = \boldsymbol{v}_t \otimes \boldsymbol{x}_s$, where $\boldsymbol{x}_t$ and $\boldsymbol{x}_s$ are (feasible) random vectors drawn from a Gaussian distribution (as in [46]) of size M and L, respectively. Results are reported in Fig. 8 where it is interesting to observe that the respective beampatterns share almost the same behavior, even if they slightly move away from the initial one while correctly keeping the nulls in the desired positions.

B. SIDELOBES ANALYSIS

To further corroborate the results of the previous subsection, herein the analysis of the sidelobes behavior is performed. In particular, the focus is again on the same interfering scenario of the first study case described by means of Figure 4(d). However, now the histograms of the sidelobes are computed having removed first the mainlobe from the related beampattern as shown in Figure 9. The areas that identify the mainbeam within the phase-only and fully-adapted beampatterns are highlighted by the green box in subplots (a) and (b), respectively, selected with the same extent in this study. Moreover, subplot (c) of the same figure compares the two sidelobes histograms. Observing these representations, the evidence is that the phase-only STAP has slightly higher sidelobes than the fully-adapted counterpart. Nevertheless, the histogram is mostly concentrated (in the simulation study) around -40 dB with respect to the peak value, that represents a quite satisfactory value within contexts of practical interest.

C. PHASES ANALYSIS

This subsection is aimed at studying the effect of quantization, i.e. impact of a finite number of bits [38, p. 287], used in the digital implementation and storage of the phase-only weight vectors. To do this, in Figure 10 the SINR values at target position are plotted as a function of the number of bits used to represent the phases in the weight vector $\boldsymbol{w}_{\mathrm{PO}}$ for the same interfering scenario as Figure 4.

The curves clearly highlight the losses suffered by the phase-only STAP receiver in utilizing a low number of bits to quantize the involved phases. Precisely, the SINR evaluated for different numbers of antenna and different numbers of pulses, viz. $(L = 8, M = 8)$, $(L = 8, M = 16)$, $(L = 16, M = 8)$, grows as the utilized number of bits increases, approximately reaching its maximum value for 10 bits. This latter represents an interesting result since the phase-only weight vector can be represented without losses with a relatively low number of bits available in commercial devices. As to the maximum SINR value observed in this figure, as highlighted before, it is essentially due to the steering of the radar toward a position different from 0 degrees and 0 Doppler.

Figure 11 depicts the behavior of the phases for the optimum phase-only STAP weight vector (and those of its competitors) considering a phased-array comprising $L = 8$ elements and transmitting a burst of $M = 8$ pulses. More specifically, Figures 11(a) to 11d) depict the contour plots of the 2D (two-dimensional) phases for the phase-only initialized with $\boldsymbol{v}$, the phase-only initialized with $\boldsymbol{w}_0 = \boldsymbol{x}_t \otimes \boldsymbol{v}_s$, the phase-only initialized with $\boldsymbol{w}_0 = \boldsymbol{v}_t \otimes \boldsymbol{x}_s$, and the phase of fully-adapted, respectively. Additionally, Figures 11(e) to 11(h) report the 2D phase difference of each studied receiving filter with respect to the nonadapted STAP. The 2D diagrams clearly highlight the phase variation over the array elements and for each considered pulse with respect to the classic counterpart.

D. PRACTICAL IMPLEMENTATION TESTS

The first test is performed to assess the validity of the Reed-Mallet-Brennan rule [36] for the phase-only STAP. The developed tests consists in evaluating the achievable SINR in a more realistic situation in which the disturbance covariance matrix is not known a-priori. In this respect, it is

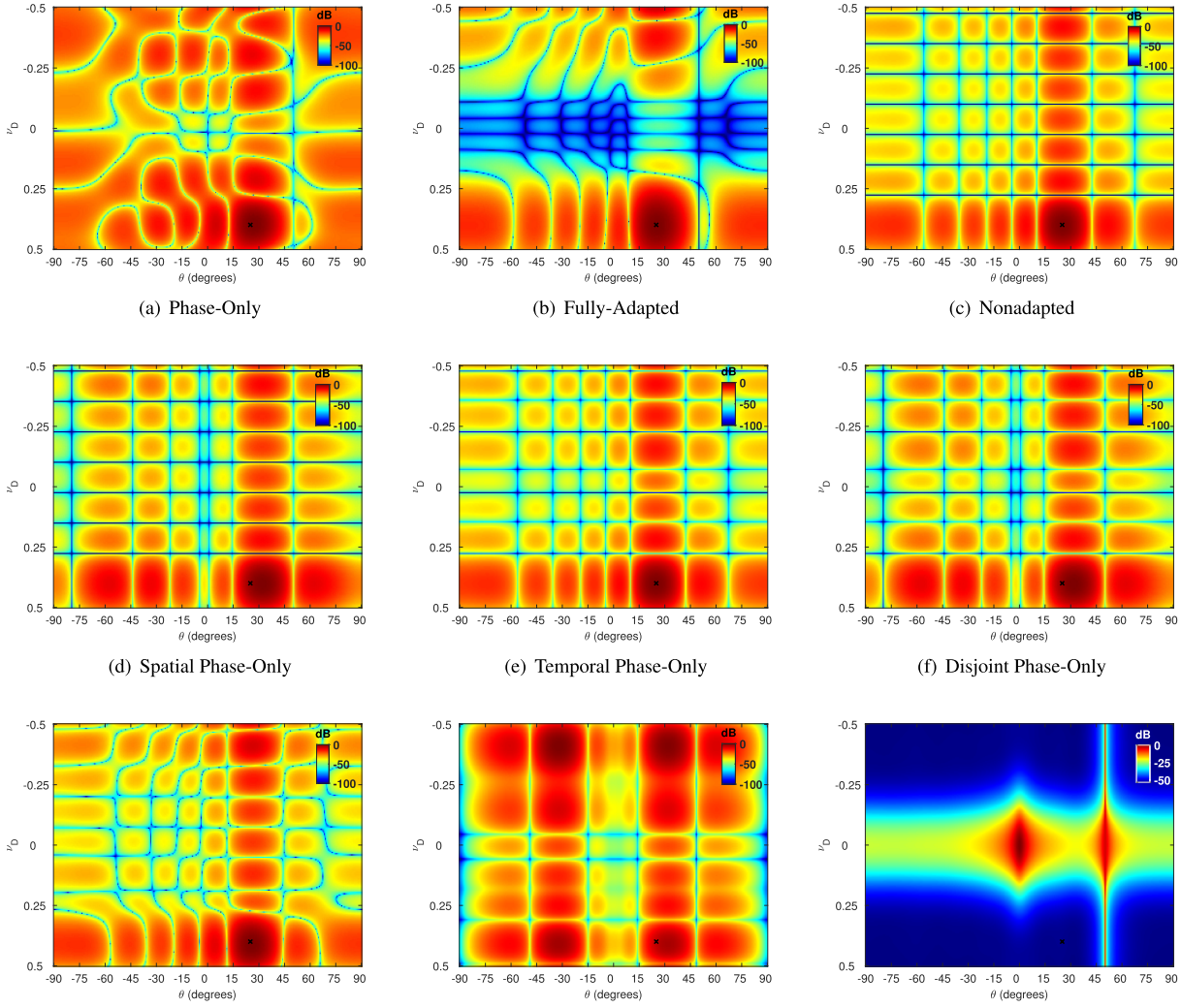

(a) Phase-Only (b) Fully-Adapted (c) Nonadapted

(d) Spatial Phase-Only (e) Temporal Phase-Only (f) Disjoint Phase-Only

(g) Fully-Adapted Phase (h) SDR (i) Interference-only

FIGURE 4. Normalized beampattern versus normalized Doppler ν_D and angle θ of the a) phase-only STAP, b) fully-adapted STAP, c) nonadapted STAP, d) spatial phase-only, e) temporal phase-only, f) disjoint phase-only STAP, g) phase of fully-adapted STAP, h) SDR of [46], and i) interference-only power.

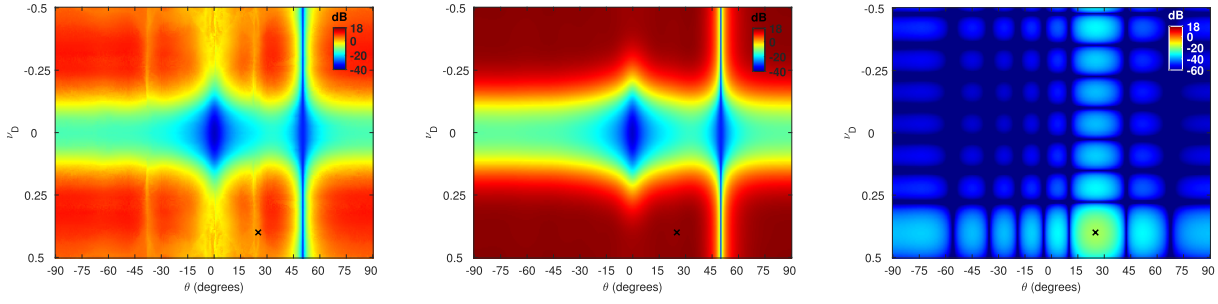

(a) Phase-Only (b) Fully-Adapted (c) Nonadapted

FIGURE 5. SINR versus normalized Doppler ν_D and angle θ of the a) phase-only STAP, b) fully-adapted STAP, and c) unadaptive STAP for the interfering scenario of Figure 4(d).

assumed the availability of range data (secondary/training data or snapshots) close to the cell under test, that are hypothesized of being stationary, homogeneous, and target free. Additionally, these data share the same statistical distribution as the primary datum, and the sample covariance matrix (SCM), that represents the maximum likelihood (ML)

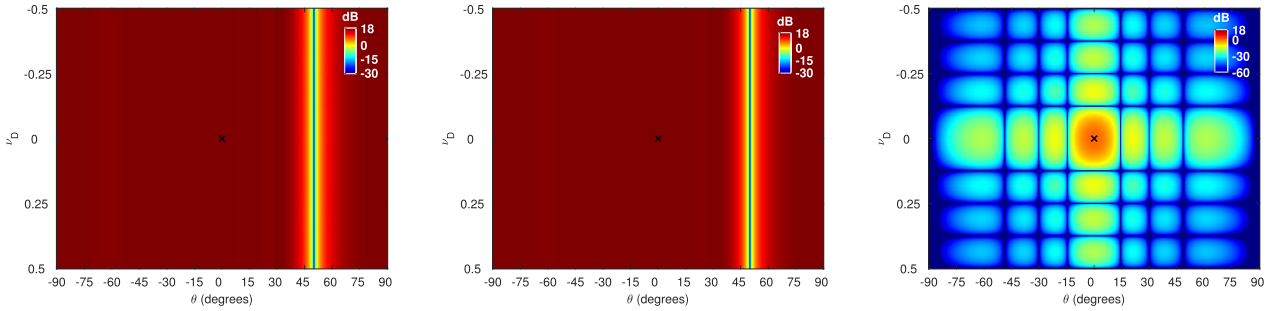

(a) Phase-Only (b) Fully-Adapted (c) Nonadapted

FIGURE 6. SINR versus normalized Doppler ν_D and angle θ of the a) phase-only STAP, b) fully-adapted STAP, and c) unadaptive STAP with the target at $\nu_{D_{tg}} = 0$ and $\theta_{tg} = 0$ degrees and interference ruled by $M = M_J + \sigma_n^2 I$.

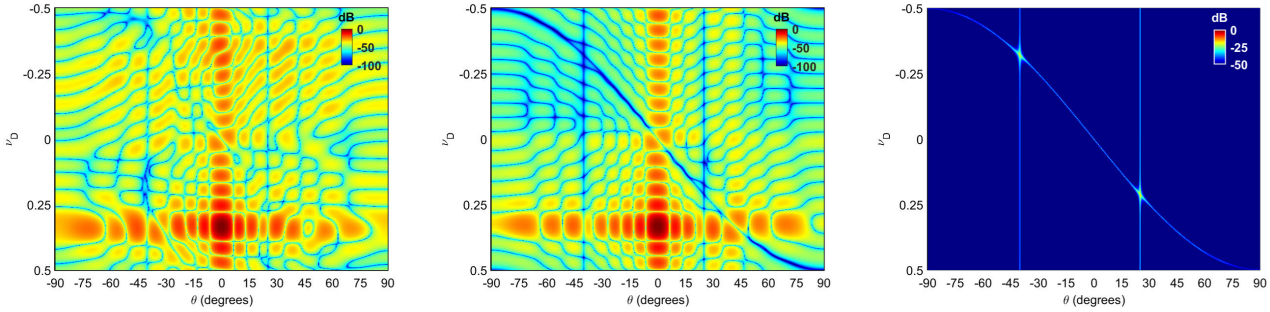

(a) Phase-Only (b) Fully-Adapted (c) Interference

FIGURE 7. Normalized beampattern versus normalized Doppler ν_D and sin of angle θ of the a) phase-only STAP and b) fully-adapted STAP, for the interfering scenario depicted in subplot c).

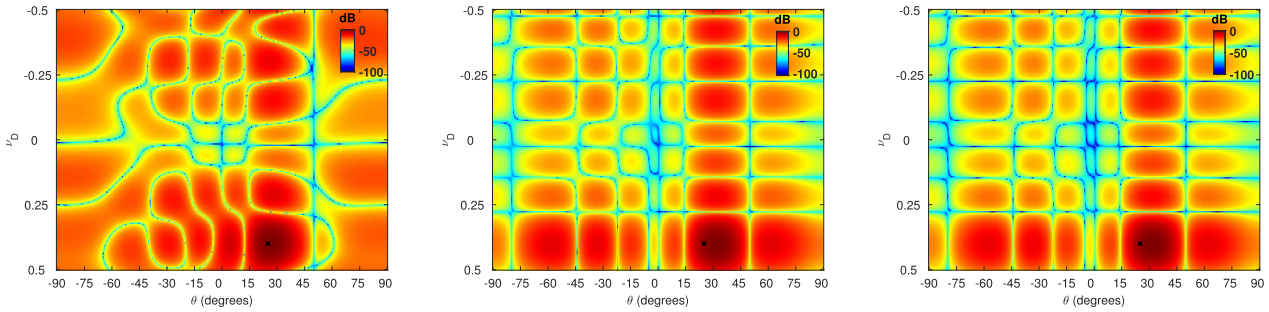

(a) $w_0 = v$ (b) $w_0 = x_t \otimes v_s$ (c) $w_0 = v_t \otimes x_s$

FIGURE 8. Normalized beampattern versus normalized Doppler ν_D and angle θ of the Phase-Only STAP with three different initializations, i.e., a) $w_0 = v$, b) $w_0 = x_t \otimes v_s$, and c) $w_0 = v_t \otimes x_s$, with x_t and x_s suitable random vectors.

estimate in homogeneous Gaussian environments [36], [47], is used in place of the true covariance in STAP evaluation.[2] For a number of snapshots approximately greater than two-times the matrix size (N herein), the SCM is capable of ensuring a SINR performance loss of only 3 dB on average with respect to the optimum [36]. After this premise, let us consider K training data, $\boldsymbol{r}_1, \ldots, \boldsymbol{r}_K$, modeled as N-dimensional independent zero-mean complex circular Gaussian vectors with the same positive definite covariance matrix $\boldsymbol{M}$ as the primary datum. Under this circumstance, the joint probability density function (pdf) of the snapshot is

$$f(\boldsymbol{r}_1, \ldots, \boldsymbol{r}_K | \boldsymbol{M}) = \frac{e^{-\mathrm{tr}\left(K\boldsymbol{M}^{-1}\boldsymbol{S}\right)}}{\pi^{NK} \det^K(\boldsymbol{M})} \tag{23}$$

where

$$\boldsymbol{S} = \frac{1}{K} \sum_{k=1}^{K} \boldsymbol{r}_k \boldsymbol{r}_k^{\dagger}. \tag{24}$$

[2] In the sample starved scenario, viz. when homogeneous secondary data are limited in number, the SCM could become ill-conditioned and more robust estimates (based for instance on diagonal loading, a-priori information or knowledge-aided as well as enforcing covariance structures) should be utilized instead. The interested reader could refer to [48]–[55], just to list a few.

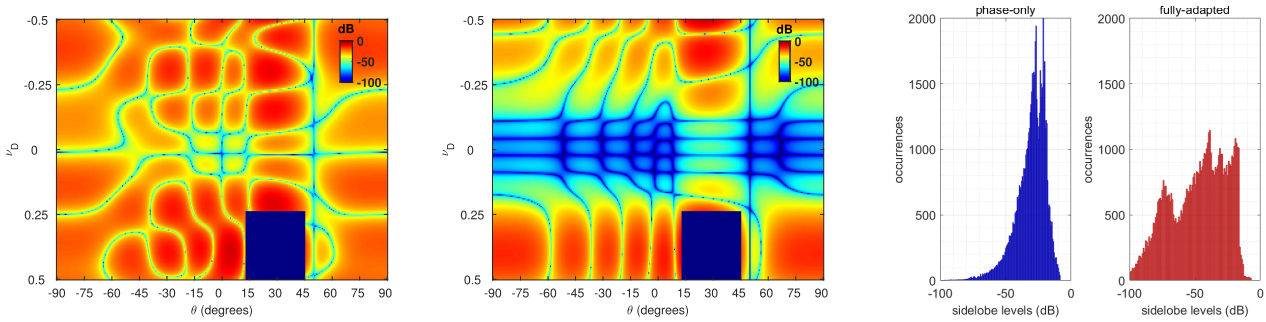

(a) Phase-Only (b) Fully-Adapted (c) Sidelobes Histograms

FIGURE 9. Sidelobes' histogram of the phase-only STAP and fully-adapted STAP. Subplots refer to a) phase-only and b) optimum-adapted SINR with emphasized the removed mainlobe for the computation of the histograms. Subplot c) instead shows the two sidelobes histograms.

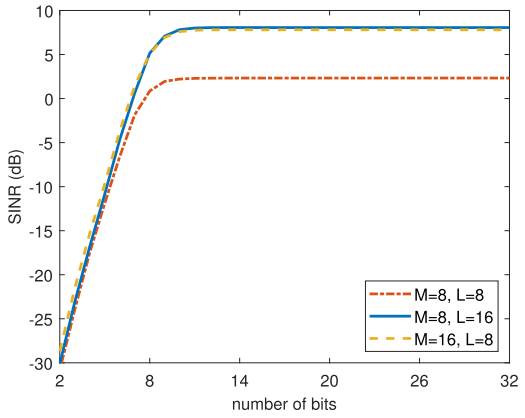

FIGURE 10. SINR at target position versus number of bits for the scenario of Figure 4.

Figure 12 shows the SINR achieved by the phase-only STAP using the SCM in place of true covariance for the interfering scenario of Figure 4(d) evaluated at the target position. The curves are plotted as function of the number of snapshots and different number of bits to quantize the phases of the estimated weight vector. From a first visual inspection, as expected, the SINR increases as the number of snapshots increases and contextually showing restrained performance losses with respect to the optimum phase-only STAP, i.e. that assuming the perfect covariance knowledge. As a matter of fact, for a number of secondary data equal to $K = 3N = 192$, the phase-only STAP with the SCM shows a SINR loss of only less than 1 dB with respect to its optimum counterpart, when a sufficient number of bits is available at the receiver. Additionally, under the challenging situation $K = N = 64$, the phase-only STAP using the SCM is able to reach SINR values whose amount of reduction is still contained in the -3 dB limit. Finally, as already observed in the analysis of Figure 10, the use of only 8 bits in the phase coding is not sufficient to provide satisfactorily performances in terms of target detection as well as interference cancellation.

Finally, we study the computational burden of the phase-only STAP considering as figure of merit the elapsed time needed to estimate the weight vector. In this respect, the test is conducted on an Intel(R) Core(TM) i5-8250U CPU @1.60GHz 1.80GHz, RAM 16 GB, whose results are graphically reported in Figure 13 varying the number of pulses (for $L = 8$ array elements) and then the number of array elements (for $M = 8$ pulses). Moreover, as for the other tests, the number of iterations for the CGM algorithm is set equal to 50, having observed that it ensures the convergence. The results emphasize that the elapsed time increases with either the number of pulses or array elements even if it is contained below 0.08 s also in the worst case. For comparison purposes, the optimum fully-adapted STAP is also considered, whose computational time is strictly related to the time needed to perform matrix inversion.

E. PHASE-ONLY STAP WITH A TRANSMITTING SLOW-TIME CODE

This section is aimed at showing the effectiveness of the phase-only STAP to generate unit-modulus weights producing space-time nulls when a specific slow-time coding $\boldsymbol{c}$ is used in transmission. To this aim, denote by $\boldsymbol{c} = [c(1), c(2), \ldots, c(M)]^T \in \mathbb{C}^M$ the transmit radar slow-time code. The signal at the receiver end is baseband-converted, undergoes a matched filter, and sampled. The N-dimensional column vector $\boldsymbol{r} = [r(1), r(2), \ldots, r(N)]^T \in \mathbb{C}^N$ of the observations in fast-time and slow-time, of the cell under test, can be expressed as

$$\boldsymbol{r} = (\boldsymbol{c} \odot \boldsymbol{v}_t(\nu_D)) \otimes \boldsymbol{v}_s(\theta) + \boldsymbol{n}. \tag{25}$$

The SINR at the receiver filter output is

$$\text{SINR} = \frac{\left|\boldsymbol{w}^\dagger \left((\boldsymbol{c} \odot \boldsymbol{v}_t(\nu_D)) \otimes \boldsymbol{v}_s(\theta)\right)\right|^2}{\boldsymbol{w}^\dagger \boldsymbol{M}_c \boldsymbol{w}}, \tag{26}$$

where the numerator is the useful energy at the output of the filter (tuned to the nominal target Doppler frequency and angular direction), while the denominator represents the signal-dependent disturbance energy at the output of the filter, with $\boldsymbol{M}_c$ the signal-dependent disturbance covariance matrix. According to the previous guidelines given in Section III, the phase-only weights $\boldsymbol{w}$ can be found using the SINR in (26) as objective function to maximize. Results of this analysis

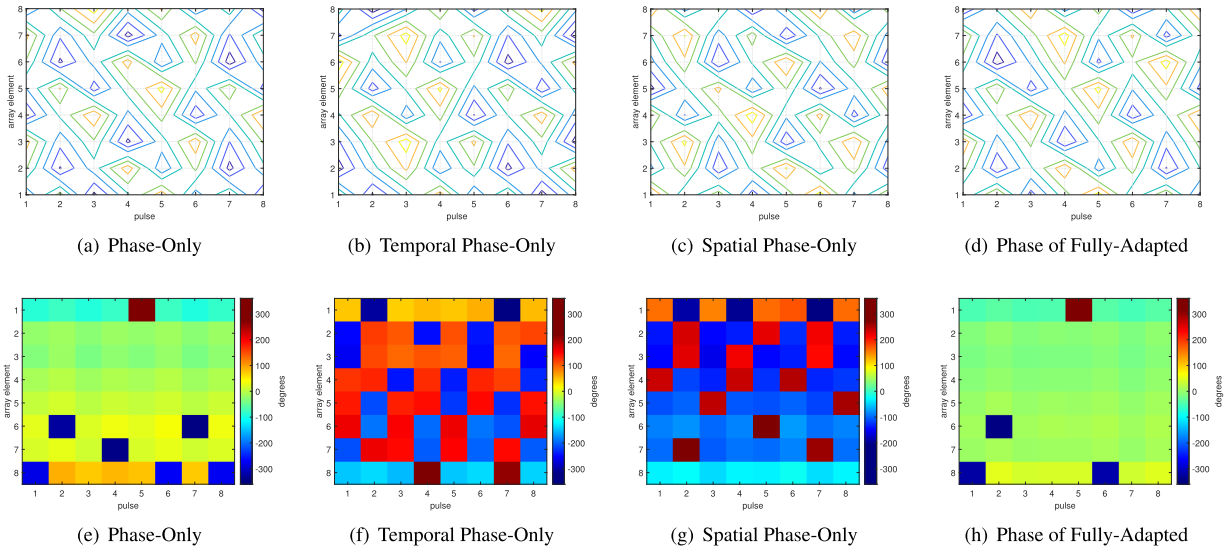

(a) Phase-Only (b) Temporal Phase-Only (c) Spatial Phase-Only (d) Phase of Fully-Adapted

(e) Phase-Only (f) Temporal Phase-Only (g) Spatial Phase-Only (h) Phase of Fully-Adapted

FIGURE 11. Phases of the STAP weight vector for an array of $L = 8$ elements transmitting $M = 8$ coherent pulses. Subplots on the top are the phases contour plot and those on bottom are the phase variation for each filter with respect to the nonadapted of a)-e) phase-only initialized with v, b)-f) phase-only initialized with $w_0 = x_t \otimes v_s$, c)-g) phase-only initialized with $w_0 = v_t \otimes x_s$, and d)-h) phase vector of fully-adapted.

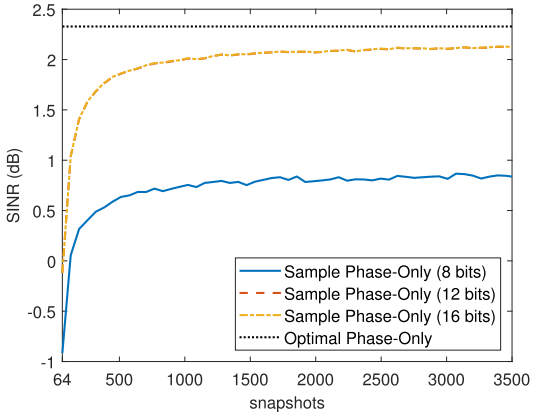

FIGURE 12. SINR versus number of snapshots, K, for a radar STAP with an array of $L = 8$ elements transmitting $M = 8$ coherent pulses, that is $N = 64$.

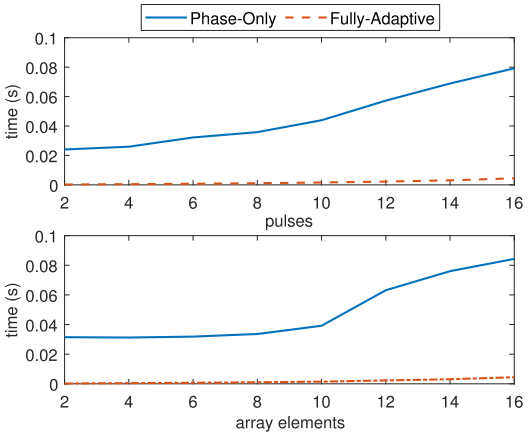

FIGURE 13. Elapsed time of the phase-only STAP for weight computation, making varying the number of antenna and the number of pulses, respectively.

are reported in Figures 14(a) to 14(c) in terms of normalized beampatterns for the phase-only STAP in comparison with the fully-adapted and the spatial phase-only previously introduced. Precisely, a radar composed by $L = 16$ array elements and transmitting a Barker code of length $M = 20$ is used. Four interfering sources from directions $\theta = [0, 10, -40, 40]$ degrees and with normalized frequencies $\nu_D = [-0.325, 0, 0.325, 0.325]$ are considered, as depicted in Figure 14(d). From figures' observation, the similarity between phase-only and fully-adapted beampatterns appears to be quite evident. Moreover, the spatial phase-only is not capable of ensuring a satisfactorily cancellation of all interferences.

F. JOINT PHASE-ONLY STAP AND TRANSMITTING WAVEFORM OPTIMIZATION

This last section provides a method for jointly optimizing the transmitted waveform and the receiving filter to improve the target detection constraining both of them to have unit-modulus (i.e., to be phase-only vectors). In particular, assuming the signals embedded in Gaussian interference, this results is achieved choosing the radar waveform and the receive filter that maximizes the SINR $\sigma(\boldsymbol{w}, \boldsymbol{p})$, that is

$$\mathcal{P}_1 \begin{cases} \arg\max_{\boldsymbol{w},\boldsymbol{p}} & \left(\dfrac{\left| \boldsymbol{w}^\dagger \boldsymbol{p} \right|^2}{\boldsymbol{w}^\dagger \boldsymbol{M} \boldsymbol{w}} \right) \\ \text{s.t.}, & \boldsymbol{w} \in \mathbb{T}^N \\ & \boldsymbol{p} \in \mathbb{T}^N, \end{cases} \tag{27}$$

where $\boldsymbol{p}$ is the radar transmitted waveform and $\boldsymbol{M}$ is the signal-independent disturbance covariance. Now, following the line of reasoning of some already published papers [25], [30], [33], [56], an iterative and alternating optimization approach is herein implemented. Precisely, at each step only

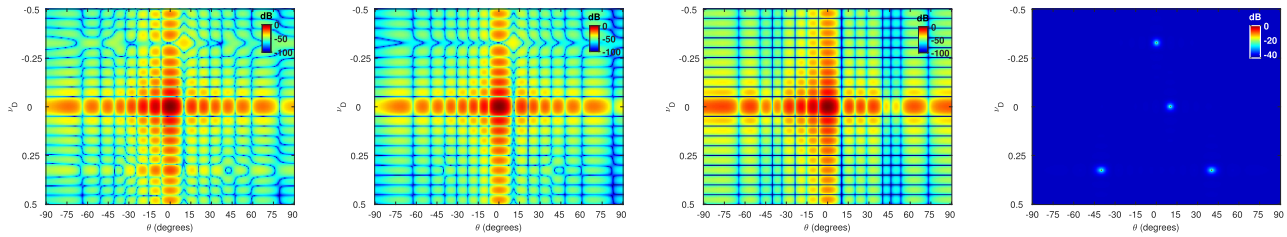

(a) Phase-Only (b) Fully-Adapted (c) Spatial Phase-Only (d) Interference-only

FIGURE 14. Normalized beampattern versus normalized Doppler ν_D and angle θ of the a) phase-only STAP, b) fully-adapted STAP, c) spatial phase-only, and d) interference-only power.

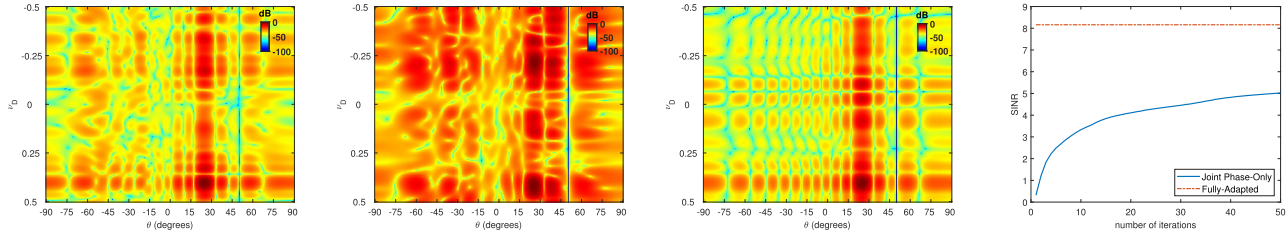

(a) Phase-Only (b) Joint Phase-Only (c) Fully-Adapted (d) SINR

FIGURE 15. Normalized beampattern versus normalized Doppler ν_D and angle θ of the a) phase-only STAP, b) joint phase-only STAP, and c) fully-adapted STAP. Subplot d) represents the achieved SINR as a function of the number of iterations in the alternating optimization.

one variable is optimized while the other is maintained fixed, and viceversa at the next step. Therefore, assuming fixed the waveform, the weight vector is optimized then, at the successive stage, the waveform is optimized maintaining fixed the weight vector optimized at the previous iterative step. Note that, the optimization of the waveform is exactly performed as described in Algorithm 1 of Section III.B, whereas that of the waveform $\boldsymbol{p}$ is done applying the phase-only CGM of Algorithm 1 with the only difference in the computation of the SINR gradient. More in details, indicating with $e^{j\boldsymbol{\Delta}}\boldsymbol{p}$ a perturbed version of the phase-only waveform $\boldsymbol{p}$, the Taylor series expansion of $\sigma(\boldsymbol{w},\boldsymbol{p})$ in (27) with respect to $\boldsymbol{\Delta}$, up to the first order, results to be

$$\sigma\left(\boldsymbol{w}, e^{j\boldsymbol{\Delta}}\boldsymbol{p}\right) = \sigma(\boldsymbol{w},\boldsymbol{p}) - j\frac{\boldsymbol{p}^{\dagger}\left[\boldsymbol{D},\boldsymbol{W}\right]\boldsymbol{p}}{\boldsymbol{w}^{\dagger}\boldsymbol{M}\boldsymbol{w}}, \tag{28}$$

where $\boldsymbol{W} = \boldsymbol{w}\boldsymbol{w}^{\dagger}$, and its gradient is

$$\nabla\sigma(\boldsymbol{w},\boldsymbol{p}) = 2\mathrm{Im}\left(\beta^{*}\boldsymbol{w}\odot\boldsymbol{c}^{*}\right)/\gamma, \tag{29}$$

where $\beta = \boldsymbol{w}^{\dagger}\boldsymbol{p}$.

The considered simulation setting comprises a disturbance covariance matrix as in (19), whereas the considered radar system is composed by an array of $L = 16$ elements and transmitting a Barker code of length $M = 20$. The starting point of the CGM is the vector $\boldsymbol{p}_0 = (\boldsymbol{c}\odot\boldsymbol{v}_t(\nu_D))\otimes\boldsymbol{v}_s(\theta)$. Figure 15 shows the normalized beampattern for the joint waveform/weight vector phase-only STAP (indicated as joint phase-only), the phase-only STAP, and the fully-adapted STAP. Interestingly, the joint phase-only put a deeper null in the jammer direction with respect to the phase-only STAP. Moreover, the SINR achieved by applying this new approach increases as the number of iteration in the alternate optimization increases, as shown in Figure 15(d).

V. CONCLUSION AND WAY AHEAD

This paper has addressed the problem of deriving the phase-only optimal weight vector for STAP. More precisely, the paper has extended a previous work [35], specifically focused on the adaptive spatial-only nulling, to the jointly space-time domain, i.e. the phase-only STAP. Differently, from the optimal fully-adapted STAP, in which the complex weight vector belongs in general to the complex field, in the phase-only STAP the weight vector is constrained to be within the so-called N-torus of phase-only complex vectors. Therefore, the problem has been formulated as a constrained maximization problem, with objective function the output SINR and with the constraint on the weight vector to be a phase-only complex vector. The solution to the corresponding constrained optimization problem has been derived by means of the phase-only CGM, due to the lack of a closed-form solution to it. Several numerical case studies have verified the effectiveness of the phase-only STAP in terms of both SINR values and receiving beampattern. The method has also been compared with the optimum fully-adapted STAP used as performance benchmark as well as other possible competitors. Finally, analyses of some practical utility have been performed to demonstrate possible pros and cons of this method.

Future research tracks might concern the application of numerical simulations in other scenarios of practical interest in the radar field as well as the validity of the proposed framework to measured radar data.

ACKNOWLEDGMENT

The authors acknowledge with thanks the fruitful discussions with Prof. Riccardo Bernardini of University of Udine (Italy) who kindly suggested the way to derive Figure 2.

REFERENCES

[1] L. E. Brennan and L. S. Reed, "Theory of adaptive radar," *IEEE Trans. Aerosp. Electron. Syst.*, vol. AES-9, no. 2, pp. 237–252, Mar. 1973.

[2] J. Ward, "Space-time adaptive processing for airborne radar," Lincoln Lab., Massachusetts Inst. Technol., Lexington, MA, USA, Tech. Rep. 1015, Dec. 1994.

[3] S. T. Smith, "Adaptive radar," in *Wiley Encyclopedia of Electrical and Electronics Engineering*. Hoboken, NJ, USA: Wiley, 2001.

[4] R. Klemm, *Principles of Space-Time Adaptive Processing*, no. 12. Edison, NJ, USA: IET, 2002.

[5] M. C. Wicks, M. Rangaswamy, R. Adve, and T. D. Hale, "Space-time adaptive processing: A knowledge-based perspective for airborne radar," *IEEE Signal Process. Mag.*, vol. 23, no. 1, pp. 51–65, Jan. 2006.

[6] E. D'Addio, A. Farina, and F. A. Studer, "Performance comparison of optimum and conventional MTI and Doppler processors," *IEEE Trans. Aerosp. Electron. Syst.*, vol. 20, no. 6, pp. 707–715, 1984.

[7] A. Farina, "STAP for SAR," in *Proc. NATO RTO Seminar (Mil. Appl. STAP)*, Istanbul, Turkey, 2002, pp. 3.1–3.23.

[8] A. Farina and P. Lombardo, *Space-Time Techniques for SAR*. London, U.K.: Institute of Engineering and Technology, 2004, ch. Applications of Space-Time Adaptive Processing.

[9] W. L. Melvin, "Space-time adaptive processing and adaptive arrays: Special collection of papers," *IEEE Trans. Aerosp. Electron. Syst.*, vol. 36, no. 2, pp. 508–509, Apr. 2000.

[10] A. Farina and L. Timmoneri, "Parallel algorithms and processing architectures for space-time adaptive processing," in *Proc. Int. Radar Conf.*, Oct. 1996, pp. 770–774.

[11] A. Farina and L. Timmoneri, "Real-time STAP techniques," in *Proc. IEE Colloq. Space-Time Adapt. Process.*, Apr. 1998, pp. 1–7.

[12] A. Farina and L. Timmoneri, "Real time STAP techniques," *ECEJ Special Issue STAP*, vol. 11, no. 1, pp. 13–22, Feb. 1999.

[13] A. Farina, "Algorithms for real-time processing," in *Proc. NATO RTO Seminar (Mil. Appl. STAP)*, Istanbul, Turkey, 2002, pp. 6.1–6.17.

[14] A. Farina and L. Timmoneri, "Parallel processing architectures for STAP," in *Applications of Space-Time Adaptive Processing*. London, U.K.: Institute of Engineering and Technology, 2004.

[15] B. Billingsley, "Impact of experimentally measured Doppler spectrum of ground clutter on MTI and STAP," in *Proc. Radar Syst. (RADAR)*, Oct. 1997, pp. 290–294.

[16] A. Farina, P. Lombardo, and M. Pirri, "Non-linear STAP processing (software tools demonstration)," in *Proc. Colloq. Digest-IEE*. London, U.K.: IEE Institution of Electrical Engineers, 1998, pp. 11–50.

[17] A. Farina, P. Lombardo, and M. Pirri, "Nonlinear STAP processing," *Electron. Commun. Eng. J.*, vol. 11, no. 1, pp. 41–48, Feb. 1999.

[18] W. L. Melvin, "Space-time adaptive radar performance in heterogeneous clutter," *IEEE Trans. Aerosp. Electron. Syst.*, vol. 36, no. 2, pp. 621–633, Apr. 2000.

[19] A. Farina and L. Timmoneri, "Cancellation of clutter and e.M. interference with STAP algorithms. Application to live data acquired with a ground-based phased array radar," in *Proc. IEEE Radar Conf.*, Apr. 2004, pp. 486–491.

[20] J. R. Guerci, J. S. Goldstein, and I. S. Reed, "Optimal and adaptive reduced-rank STAP," *IEEE Trans. Aerosp. Electron. Syst.*, vol. 36, no. 2, pp. 647–663, Apr. 2000.

[21] C. D. Peckham, A. M. Haimovich, T. F. Ayoub, J. S. Goldstein, and I. S. Reid, "Reduced-rank STAP performance analysis," *IEEE Trans. Aerosp. Electron. Syst.*, vol. 36, no. 2, pp. 664–676, Apr. 2000.

[22] K. Gerlach and M. L. Picciolo, "Airborne/spacebased radar STAP using a structured covariance matrix," *IEEE Trans. Aerosp. Electron. Syst.*, vol. 39, no. 1, pp. 269–281, Jan. 2003.

[23] W. L. Melvin and G. A. Showman, "An approach to knowledge-aided covariance estimation," *IEEE Trans. Aerosp. Electron. Syst.*, vol. 42, no. 3, pp. 1021–1042, Jul. 2006.

[24] P. Stoica, J. Li, X. Zhu, and J. R. Guerci, "On using a priori knowledge in space-time adaptive processing," *IEEE Trans. Signal Process.*, vol. 56, no. 6, pp. 2598–2602, Jun. 2008.

[25] A. Aubry, A. DeMaio, A. Farina, and M. Wicks, "Knowledge-aided (potentially cognitive) transmit signal and receive filter design in signal-dependent clutter," *IEEE Trans. Aerosp. Electron. Syst.*, vol. 49, no. 1, pp. 93–117, Jan. 2013.

[26] A. K. Shackelford, K. Gerlach, and S. D. Blunt, "Partially adaptive STAP using the FRACTA algorithm," *IEEE Trans. Aerosp. Electron. Syst.*, vol. 45, no. 1, pp. 58–69, Jan. 2009.

[27] A. De Maio, S. De Nicola, Y. Huang, D. P. Palomar, S. Zhang, and A. Farina, "Code design for radar STAP via optimization theory," *IEEE Trans. Signal Process.*, vol. 58, no. 2, pp. 679–694, Feb. 2010.

[28] G. Ginolhac, P. Forster, F. Pascal, and J.-P. Ovarlez, "Performance of two low-rank STAP filters in a heterogeneous noise," *IEEE Trans. Signal Process.*, vol. 61, no. 1, pp. 57–61, Jan. 2013.

[29] M. Yang, A. De Maio, and Y. Huang, "Efficient algorithms for robust factored radar STAP," in *Proc. IEEE 8th Int. Workshop Comput. Adv. Multi-Sensor Adapt. Process. (CAMSAP)*, Dec. 2019, pp. 510–514.

[30] B. Tang and J. Tang, "Joint design of transmit waveforms and receive filters for MIMO Radar space-time adaptive processing," *IEEE Trans. Signal Process.*, vol. 64, no. 18, pp. 4707–4722, Sep. 2016.

[31] G. Cui, X. Yu, V. Carotenuto, and L. Kong, "Space-time transmit code and receive filter design for colocated MIMO radar," *IEEE Trans. Signal Process.*, vol. 65, no. 5, pp. 1116–1129, 2017.

[32] L. Wu, P. Babu, and D. P. Palomar, "Transmit waveform/receive filter design for MIMO radar with multiple waveform constraints," *IEEE Trans. Signal Process.*, vol. 66, no. 6, pp. 1526–1540, May 2018.

[33] B. Tang, J. Tuck, and P. Stoica, "Polyphase waveform design for MIMO radar space time adaptive processing," *IEEE Trans. Signal Process.*, vol. 68, pp. 2143–2154, Mar. 2020.

[34] S. M. O'Rourke, P. Setlur, M. Rangaswamy, and A. L. Swindlehurst, "Quadratic semidefinite programming for waveform-constrained joint filter-signal design in STAP," *IEEE Trans. Signal Process.*, vol. 68, pp. 1744–1759, Mar. 2020.

[35] S. T. Smith, "Optimum phase-only adaptive nulling," *IEEE Trans. Signal Process.*, vol. 47, no. 7, pp. 1835–1843, Jul. 1999.

[36] I. S. Reed, J. D. Mallett, and L. E. Brennan, "Rapid convergence rate in adaptive arrays," *IEEE Trans. Aerosp. Electron. Syst.*, vol. AES-10, no. 6, pp. 853–863, Nov. 1974.

[37] M. R. Hestenes and E. Stiefel, "Methods of conjugate gradients for solving linear systems," *J. Res. Nat. Bureau Standards*, vol. 49, no. 6, pp. 409–436, Dec. 1952.

[38] A. Farina, *Antenna-Based Signal Processing Techniques for Radar Systems*. Norwood, MA, USA: Artech House, 1992.

[39] C. Baird and G. Rassweiler, "Adaptive sidelobe nulling using digitally controlled phase-shifters," *IEEE Trans. Antennas Propag.*, vol. AP-24, no. 5, pp. 638–649, Sep. 1976.

[40] A. Edelman, T. A. Arias, and S. T. Smith, "The geometry of algorithms with orthogonality constraints," *SIAM J. Matrix Anal. Appl.*, vol. 20, no. 2, pp. 303–353, 1998.

[41] S. T. Smith, "Optimization techniques on Riemannian manifolds," *Fields Inst. Commun.*, vol. 3, no. 3, pp. 113–135, 1994.

[42] S. T. Smith, "Conjugate gradient and Newton methods for optimal phase-only adaptive nulling," in *Proc. Adapt. Antenna Syst. Symp.*, Nov. 1994, pp. 2–8.

[43] S. T. Smith, "Geometric optimization methods for adaptive filtering," Ph.D. dissertation, Division Appl. Sci., Harvard Univ., Cambridge, MA, USA, 1993.

[44] C. F. Van Loan and G. H. Golub, *Matrix Computations*. Baltimore, MD, USA: Johns Hopkins University Press Baltimore, 1983.

[45] S. T. Smith, "Performance of optimum phase-only adaptive nulling algorithms," in *Proc. Int. Symp. Phased Array Syst. Technol.*, Oct. 1996, pp. 353–358.

[46] C.-J. Lu, W.-X. Sheng, Y.-B. Han, and X.-F. Ma, "A novel adaptive phase-only beamforming algorithm based on semidefinite relaxation," in *Proc. IEEE Int. Symp. Phased Array Syst. Technol.*, Oct. 2013, pp. 617–621.

[47] F. C. Robey, D. R. Fuhrmann, E. J. Kelly, and R. Nitzberg, "A CFAR adaptive matched filter detector," *IEEE Trans. Aerosp. Electron. Syst.*, vol. 28, no. 1, pp. 208–216, Jan. 1992.

[48] A. Farina, P. A. Langsford, G. C. Sarno, L. Timmoneri, and R. Tosini, "ECCM techniques for a rotating, multifunction, phased-array radar," in *Proc. 25th Eur. Microw. Conf.*, Oct. 1995, pp. 490–495.

[49] M. Steiner and K. Gerlach, "Fast converging adaptive processor or a structured covariance matrix," *IEEE Trans. Aerosp. Electron. Syst.*, vol. 36, no. 4, pp. 1115–1126, Oct. 2000.

[50] Y. Chen, A. Wiesel, Y. C. Eldar, and A. O. Hero, "Shrinkage algorithms for MMSE covariance estimation," *IEEE Trans. Signal Process.*, vol. 58, no. 10, pp. 5016–5029, Oct. 2010.

[51] A. Aubry, A. D. Maio, L. Pallotta, and A. Farina, "Radar detection of distributed targets in homogeneous interference whose inverse covariance structure is defined via unitary invariant functions," *IEEE Trans. Signal Process.*, vol. 61, no. 20, pp. 4949–4961, Oct. 2013.

[52] O. Besson and Y. I. Abramovich, "Regularized covariance matrix estimation in complex elliptically symmetric distributions using the expected likelihood approach—Part 2: The under-sampled case," *IEEE Trans. Signal Process.*, vol. 61, no. 23, pp. 5819–5829, Dec. 2013.
[53] A. Aubry, A. D. Maio, and L. Pallotta, "A geometric approach to covariance matrix estimation and its applications to radar problems," *IEEE Trans. Signal Process.*, vol. 66, no. 4, pp. 907–922, Feb. 2018.
[54] V. Carotenuto, A. De Maio, D. Orlando, and L. Pallotta, "Adaptive radar detection using two sets of training data," *IEEE Trans. Signal Process.*, vol. 66, no. 7, pp. 1791–1801, Apr. 2018.
[55] A. De Maio, L. Pallotta, J. Li, and P. Stoica, "Loading factor estimation under affine constraints on the covariance eigenvalues with application to radar target detection," *IEEE Trans. Aerosp. Electron. Syst.*, vol. 55, no. 3, pp. 1269–1283, Jun. 2019.
[56] A. Aubry, V. Carotenuto, A. De Maio, A. Farina, and L. Pallotta, "Optimization theory-based radar waveform design for spectrally dense environments," *IEEE Aerosp. Electron. Syst. Mag.*, vol. 31, no. 12, pp. 14–25, Dec. 2016.

LUCA PALLOTTA (Senior Member, IEEE) received the Laurea Specialistica degree *(cum laude)* in telecommunication engineering from the University of Sannio, Benevento, Italy, in 2009, and the Ph.D. degree in electronic and telecommunication engineering from the University of Naples Federico II, Naples, Italy, in 2014. He is currently an Assistant Professor with the University of Roma Tre, Italy. His research interests include statistical signal processing, with emphasis on radar/SAR signal processing, radar targets detection and classification, and polarimetric radar/SAR. He has won the Student Paper Competition at the 2013 IEEE Radar Conference. Since November 2020, he has been an Associate Editor for IEEE JOURNAL OF SELECTED TOPICS IN APPLIED EARTH OBSERVATIONS AND REMOTE SENSING (JSTARS). From July 2018 to February 2021, he was an Associate Editor for the journal *Signal, Image and Video Processing* (SIVP) (Springer).

ALFONSO FARINA (Life Fellow, IEEE) received the D.Ing. degree in electronic engineering from the University of Rome, Rome, Italy, in 1973.

In 1974, he joined Selex ES (formerly Selenia), Rome, where he became the Director of the Analysis of Integrated Systems Unit and subsequently the Director of Engineering of the Large Business Systems Division. In 2012, he was a Senior VP and a Chief Technology Officer of the company, reporting directly to the President. From 2013 to 2014, he was a Senior Advisor to the CTO. He retired in October 2014. From 1979 to 1985, he was also a Professor of radar techniques with the University of Naples Federico II, Naples, Italy. He is the author of more than 800 peer-reviewed technical publications, books, and monographs published worldwide, some of them also translated into Russian and Chinese. He is currently a Visiting Professor with the University College London, London, U.K., and Cranfield University, Cranfield, U.K., and the Académico Correspondiente de la Real Academia de Ingeniería de España.

Dr. Farina is also a member of the European Academy of Science. Since 2019, he has been a member of the IEEE Aerospace and Electronic Systems Society (AESS) Board of Governors. He is also a fellow of IET; the Royal Academy of Engineering, U.K., in 2005; and the European Association for Signal Processing (EURASIP). He was a recipient of the Fred Nathanson Memorial Radar Award, in 1987; the Finmeccanica Award for Innovation Technology, in 2004; the IEEE Dennis J. Picard Medal for Radar Technologies and Applications, in 2010; the Oscar Masi Award, in 2012; the IET Achievement Medal, in 2014; the IEEE SPS Industrial Leader Award, in 2017; the Christian Hülsmeyer Award, in 2019; and the IEEE AESS Pioneer Award, in 2020. His main best paper awards include the B. Carlton of IEEE TRANSACTIONS ON AEROSPACE AND ELECTRONIC SYSTEMS, in 2001, 2003, and 2013; the *IET Proceedings on Radar Sonar and Navigation*, in 2009 and 2010; and the International Conference on Fusion, in 2005.

STEVEN THOMAS SMITH (Fellow, IEEE) received the B.A.Sc. degree (Hons.) in electrical engineering and mathematics from The University of British Columbia, Vancouver, BC, Canada, in 1986, and the Ph.D. degree in applied mathematics from Harvard University, Cambridge, MA, USA, in 1993. He is an expert in radar, sonar, and signal processing who has made pioneering and wide ranging contributions through his research and technical leadership in estimation theory, resolution limits, and signal processing and optimization on manifolds. He has more than 20 years experience as an Innovative Technology Leader with statistical data analytics, both theory and practice, and broad leadership experience ranging from first-of-a-kind algorithm development for groundbreaking sensor systems to graph-based intelligence architectures. His contributions span diverse applications from optimum network detection, geometric optimization, geometric acoustics, super resolution, and nonlinear parameter estimation. He was a recipient of the SIAM Outstanding Paper Award, in 2001, and the IEEE Signal Processing Society Best Paper Award, in 2010. He has been an invited speaker as an original inventor of some of the big advances in signal processing over the last decade. He was an Associate Editor of the IEEE TRANSACTIONS ON SIGNAL PROCESSING, from 2000 to 2002, and serves on the IEEE Sensor Array and Multichannel Technical Committee and IEEE Big Data Technical Committee. He has taught signal processing courses at Harvard, MIT, and for the IEEE. He is a Senior Staff Member with the MIT Lincoln Laboratory.

GAETANO GIUNTA (Senior Member, IEEE) received the degree in electronic engineering from the University of Pisa, Italy, in 1985, and the Ph.D. degree in information and communication engineering from the University of Rome La Sapienza, Italy, in 1990. Since 1989, he has been a Research Fellow of the Signal Processing Laboratory (LTS), EPFL, Lausanne, Switzerland. In 1992, he became an Assistant Professor with the INFO-COM Department, University of Rome La Sapienza. From 2001 to 2005, he was with the Third University of Rome as an Associate Professor, where he has been a Full Professor of telecommunications, since 2005. His research interests include signal processing for mobile communications, image communications, and security. He has been a member of the IEEE Societies of Communications, Signal Processing, and Vehicular Technology. He has also served as a Reviewer for several IEEE TRANSACTIONS, IET (formerly IEE) proceedings, and EURASIP journals, and a TPC member for several international conferences and symposia in the same fields.